

A. J. Tuononen and M. J. Matilainen. 2009. Real-time estimation of aquaplaning with an optical tyre sensor. Proceedings of the Institution of Mechanical Engineers, Part D: Journal of Automobile Engineering, volume 223, number D10, pages 1263-1272.

© 2009 Professional Engineering Publishing

Reprinted with permission.

# Real-time estimation of aquaplaning with an optical tyre sensor

A J Tuononen\* and M J Matilainen

Laboratory of Automotive Engineering, Helsinki University of Technology, TKK, Finland

*The manuscript was received on 23 March 2009 and was accepted after revision for publication on 4 June 2009.*

DOI: 10.1243/09544070JAUTO1220

**Abstract:** Future active safety systems will require more accurate information about the state of a vehicle and the operating conditions of an individual tyre. Aquaplaning is a dangerous situation in which the contact between the tyre and the road is partially or completely lost. In this paper, the movements of the inner liner of the tyre during aquaplaning are measured optically and exploited to estimate aquaplaning. The results from proving-ground tests are shown and compared with those of the conventional approach of estimating aquaplaning from wheel speeds. The proposed method performs reliably in real time and can detect several different levels of aquaplaning. The results support the future development of production-capable tyre sensors. An optical tyre sensor also provides a research tool for attaining an in-depth understanding of the aquaplaning phenomenon.

**Keywords:** tyre sensor, aquaplaning, hydroplaning, driver assistance system, active safety system

## 1 INTRODUCTION

The primary function of a vehicle tyre is to provide the interface between the vehicle and the road surface. The apparent rubber contact area of a typical mid-size vehicle tyre against the road surface is about the same as the area of a man's palm. All the significant forces and moments that act on a vehicle, besides gravity and aerodynamic forces, are generated through these relatively tiny contact patches. Aquaplaning is a phenomenon where the contact between the tyre and the road surface is partially or completely lost.

The first studies concerning aquaplaning were conducted between the years 1950 and 1960 by NASA. Back in those days, jet-powered aircraft were becoming common in the USA's commercial airline traffic. The higher take-off and landing velocities required for the new big jet airplanes, along with their lower acceleration characteristics, presented

problems with runways covered with water or slush [1].

Between the years 1960 and 1980, the studies concentrated mainly on crossply tyres. It is obvious that these studies cannot be applied directly to modern radial tyres because of the different tyre characteristics. However, many fundamental ideas and calculation models of aquaplaning were developed in this period of time.

Figure 1 represents the classical three-zone model, which divides the contact patch of an aquaplaning tyre into three different zones. In zone A, the inertial effect of the water dominates, the hydrodynamic pressure overcomes the tyre's contact pressure, and there is no contact between the tyre and the road surface. In zone B, the viscous effect of water squeezing out from the contact area limits the grip of this region. The viscous aquaplaning phenomenon is very similar to, for example, the lubrication of a bearing. Consequently, water forms a thin layer between the tyre and the road surface, which reduces the friction substantially. However, the microroughness of the road surface breaks the water layer and provides some contact with the tyre. Hence, the roughness of the road surface is abso-

\*Corresponding author: Laboratory of Automotive Engineering, Helsinki University of Technology, P.O. Box 4300, TKK, 02015, Finland.

email: ari.tuononen@tkk.fi

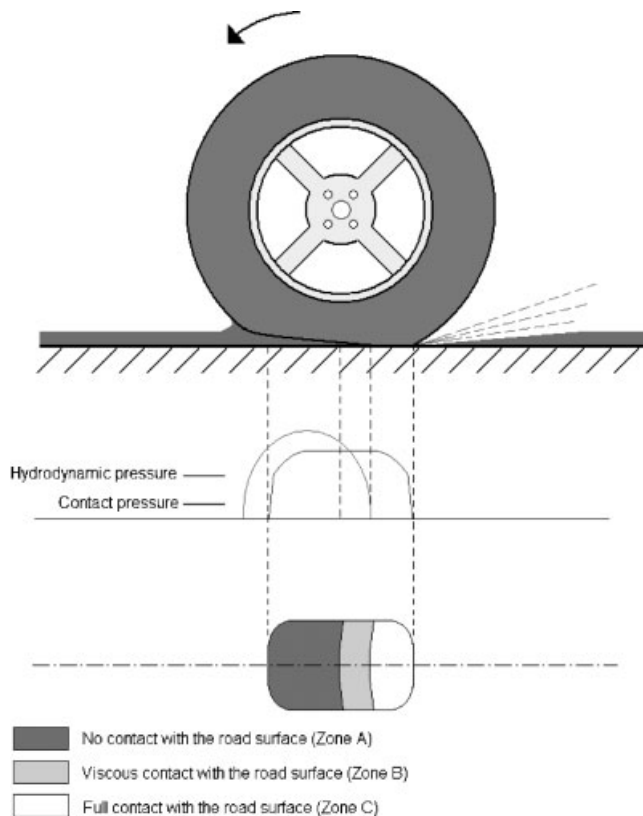


Fig. 1 Three-zone model

lutely crucial for viscous aquaplaning. In zone C, the tyre contacts the damp road completely [2, 3].

The present electronic stability control (ESC) active safety systems and upcoming advanced driver assistance system (ADAS) applications are quite vulnerable to special situations such as aquaplaning. Failure to recognize these situations correctly can mislead state estimators of active systems and, in the worst case, cause life-threatening collisions or other hazards. For example, if a vehicle is spinning and the tyre for ESC brake intervention is aquaplaning, the vehicle will not stabilize. If the aquaplaning status of each tyre were known, the ESC could choose the second-best, but non-aquaplaning, tyre for the brake intervention [4].

Because aquaplaning has a very sudden impact on the controllability of vehicles, it is vitally important to be able to detect an aquaplaning situation while it is still only partial. The wheel speed sensors that currently exist cannot identify aquaplaning very precisely, and certainly not its early stages. If there were a system that could estimate a partial aquaplaning situation, it would be possible to warn the driver with an aquaplaning warning signal. With this information, the driver could slow down before the tyre was fully aquaplaning. The partial aquaplan-

ing information would also be very important for systems such as adaptive cruise control (ACC). The ACC system could increase the distance from the vehicle driving ahead when partial aquaplaning was detected.

There have not been any studies regarding the real-time estimation of aquaplaning by means of a tyre sensor. However, the University of Darmstadt in Germany has done some aquaplaning research with tyre sensors. The Darmstadt tyre sensor measured tread block deformations and could detect two points: the beginning of the contact with the water and the leading edge of the contact with the road surface. The Darmstadt tyre sensor was not used for the real-time estimation of aquaplaning [5].

The objective of the present work was to develop real-time estimation software for aquaplaning by measuring tyre carcass deflection with an optical sensor. The real-time estimation software was verified through proving-ground tests.

## 2 OPTICAL TYRE SENSOR (OTS)

The optical tyre sensor was developed in two EC-funded projects (Apollo 2002–2005 and FRICTI@N 2006–2008). The Apollo project investigated three different types of sensor: a piezoelectric deformation sensor, a three-axis accelerometer, and a three-axis optical sensor. All of these sensors were assembled in the inner liner of the tyre. The FRICTI@N project continued to develop the three-axis optical sensor further [6, 7].

The main components of the OTS are a two-dimensional photosensitive detector (PSD) and a wide-angle light-emitting diode (LED). The PSD is located on the rim and the LED is installed in the inner liner of the tyre. The PSD utilizes the photodiode surface resistance and can measure the movement of the LED with respect to the rim. In front of the PSD there is a lens with an antireflection coating, which focuses the light on the sensor. The effective focal length of the lens is 9 mm, and that is also the distance from the PSD to the lens [7]. When a spot of light strikes the PSD, an electric charge proportional to the light intensity is generated at the incident position. This electric charge is driven through the resistive layer and collected by the output electrodes as photocurrents [8].

The data from the PSD are digitized in a 12-bit AD converter and transmitted wirelessly to the receiver at 433 MHz. After the receiver, the digitized data are demodulated and transformed to CAN message format. A Li-Ion battery serves as a power supply.

There is also an inductive sensor on the rim aligned with the optical sensor, which synchronizes the tyre sensor data with the rotation angle when it passes the magnet in the suspension. The assembly of the optical tyre sensor is illustrated in Fig. 2 [7].

The vertical movement of the tyre carcass with respect to the rim can be determined from the intensity signal of the OTS. When the vehicle is being driven at a constant speed on dry flat tarmac, the LED on the inner liner is closest to the rim around the bottom dead centre (BDC) (Fig. 3). During aquaplaning, the hydrodynamic pressure is greater than the local pressure of the tyre on the road surface. This causes the leading edge of the tyre to lift off the road surface, and hence the LED on the inner liner is closer to the rim before the BDC (Fig. 3). By calculating the centroid (centre of mass (CM)) position of the intensity signal from each rotation, the situation when the tyre is aquaplaning can be estimated.

Figure 4 illustrates the weighted mean curves of the intensity signal from one test run at an aquaplaning proving ground. The curves with circular markers represent the situation before the water reservoir (dry tarmac and constant speed), and the curves with plus markers represent the aquaplaning situation.

The real-time estimation software of aquaplaning was tested at an aquaplaning proving ground (flooded, water depth roughly 8 mm). The tyre used

in the test was a non-studded Nokian WR 205/55R16 91 H Central European winter tyre (rather new, tread depth  $\sim 7$  mm, inflated to 2.5 bar). The optical tyre was fitted to the front left corner of the test vehicle (VW Golf V Variant 1.9 TDI). The tests followed the same pattern. First, the vehicle was accelerated to the desired constant speed (60, 70, 80, 90, and 100 km/h), and, just before the water reservoir (depth of water  $\sim 8$  mm), the clutch was depressed. However, the estimation was also tested without the clutch being depressed, and it was tested in FWD and 4WD cars to verify robustness of the algorithm. Similarly, the estimation performed well with summer tyre Hakka H 205/55R16 94 H, but these results are not presented here.

### 3 REAL-TIME ESTIMATION OF AQUAPLANING

The real-time estimation software for aquaplaning was developed with Matlab/Simulink software (MathWorks, Inc.). The Simulink model was compiled to an executable file and uploaded to a rapid prototyping computer. The user interface was created with ControlDesk software (dSPACE), which illustrated the estimated aquaplaning percentage and other relevant information (Fig. 5).

It was quite obvious in the early stages of the development process that the best way to estimate aquaplaning was from either the vertical or the

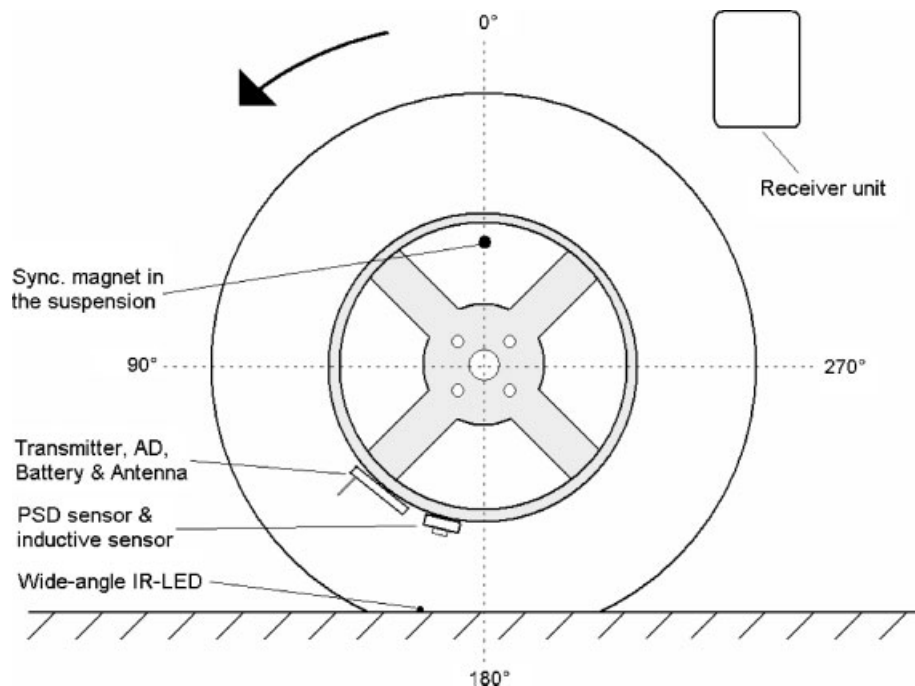


Fig. 2 Optical tyre sensor assembly

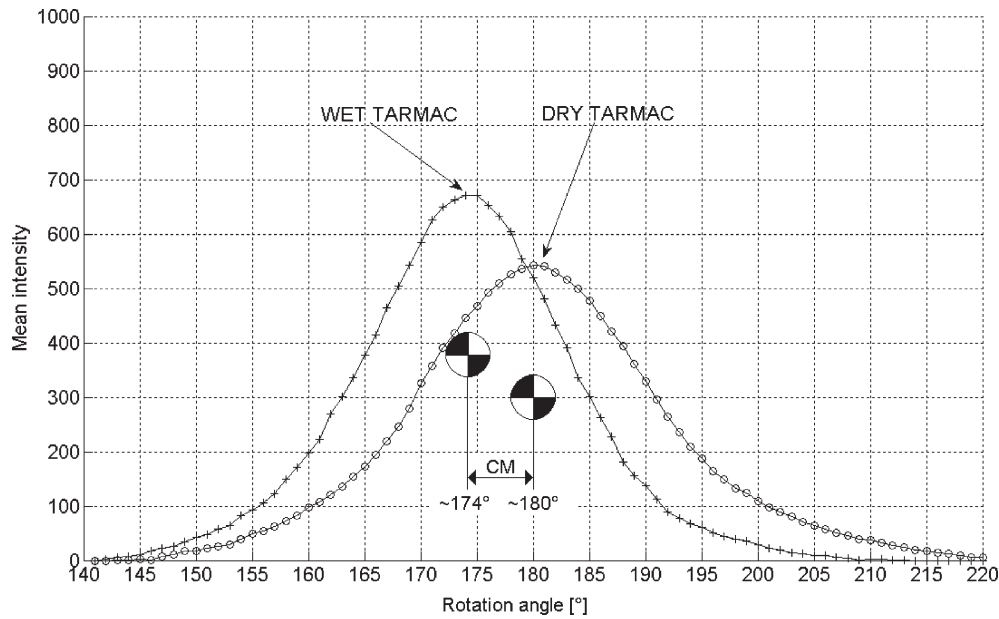


Fig. 3 Principle of the real-time estimation of aquaplaning

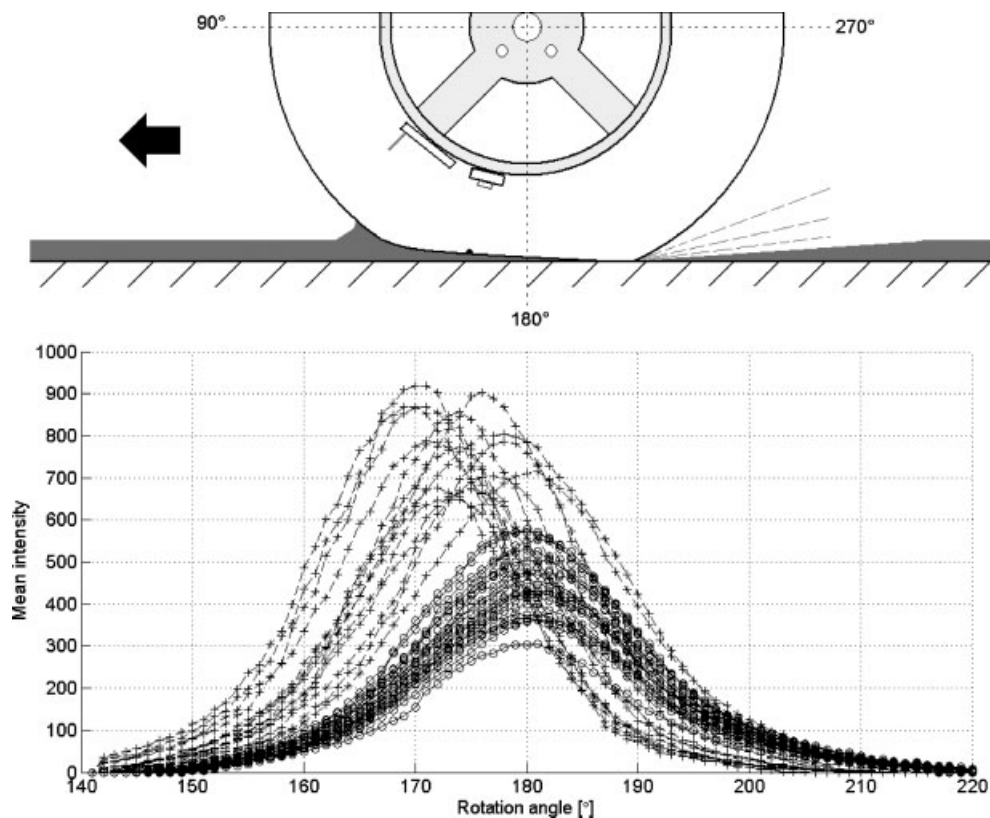


Fig. 4 Weighted mean curves of the intensity signal (dry tarmac: lines with circular markers; wet tarmac: lines with plus markers)

longitudinal signal of the PSD sensor. Previous track tests with the optical tyre sensor had shown that both of these signals changed substantially when the vehicle was driven into a water reservoir [4].

Different algorithms to estimate aquaplaning from both of these signals were investigated in the simulation phase of the development process. The most promising of these algorithms proved to be

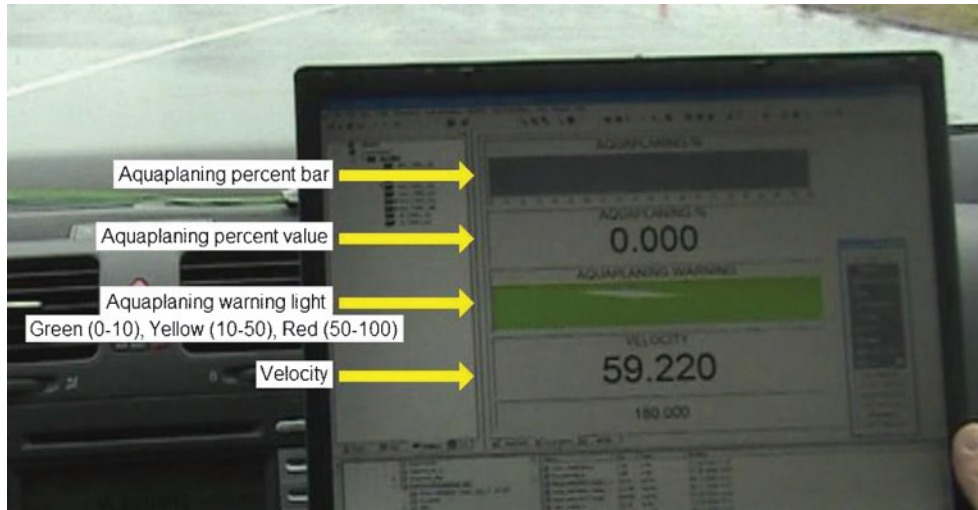


Fig. 5 Demonstration layout for real-time estimation of aquaplaning

calculating the weighted mean of the intensity signal from five recent rotations and comparing the shifting of this signal on the rotational axis (Fig. 3).

The whole real-time aquaplaning estimation process is illustrated in Fig. 6. The aquaplaning estimation block takes input from three different sources: the optical tyre sensor (OTS), the internal measurement unit (IMU), and the vehicle CAN bus. The OTS provides the three-dimensional movement information (vertical, longitudinal, and lateral) of the inner liner of the tyre to the estimation block. However, only the vertical signal of the OTS is used for the estimation. The inductive sensor is used to identify when the OTS is in the top dead centre (TDC) position. The TDC information of the OTS is needed for timing the collection of OTS data from one rotation into a vector form and triggering the subsystem where most of the calculations are performed. The data from the inductive sensor have the same signal path as the OTS.

The longitudinal acceleration and vehicle speed are exploited in activating the estimation in suitable conditions such as when vehicle speed is over 14 m/s and longitudinal acceleration remains under 0.1 g. In this situation, aquaplaning is possible and braking and accelerating do not disturb the tyre sensor signal. The brake pressure information could also be used for the activation.

The whole aquaplaning estimation process is based on comparing the OTS intensity data from different rotations. This is why the data from each rotation are collected into vector form. The aquaplaning estimation block can be run during a time step (0.2 ms), and therefore multitasking is not required. The amount of samples collected from one rotation depends on the velocity of the vehicle

(Fig. 7). The faster the vehicle is moving, the fewer the number of samples per rotation that are attained, and vice versa. However, in Simulink, the length of the vector cannot be dynamic, and therefore the input vector has to be initialized to some static length. The length of the input vector was chosen to be 1200, which is sufficient for velocities greater than 30 km/h. Equation (1) shows how many samples are attained per rotation as a function of velocity

$$s_a(v) = \frac{s_r c}{v} \quad (1)$$

where  $s_r$  is the sample rate,  $c = 2\pi r_d$  is the circumference of the tyre,  $r_d$  is the dynamic rolling radius of the tyre, and  $v$  is the velocity of the vehicle.

The update rate of the intensity data (a data vector of complete rotation) increases in a linear fashion as a function of velocity

$$u_r(v) = \frac{v}{c} \quad (2)$$

In order to compare the intensity data from different rotations, the data have to be interpolated to a polar coordinate system (0–360°). Before this can be done, the actual number of data points from the current rotation (marked as  $l$  in equation (3)) has to be determined. Equation (3) defines the corresponding index points of the input vector to the polar coordinate system. By rounding the value that equation (3) assigns down and up, the interpolation (equation (6)) can be executed between these two points

$$e(k) = k \left( \frac{l}{360} \right) \quad (3)$$

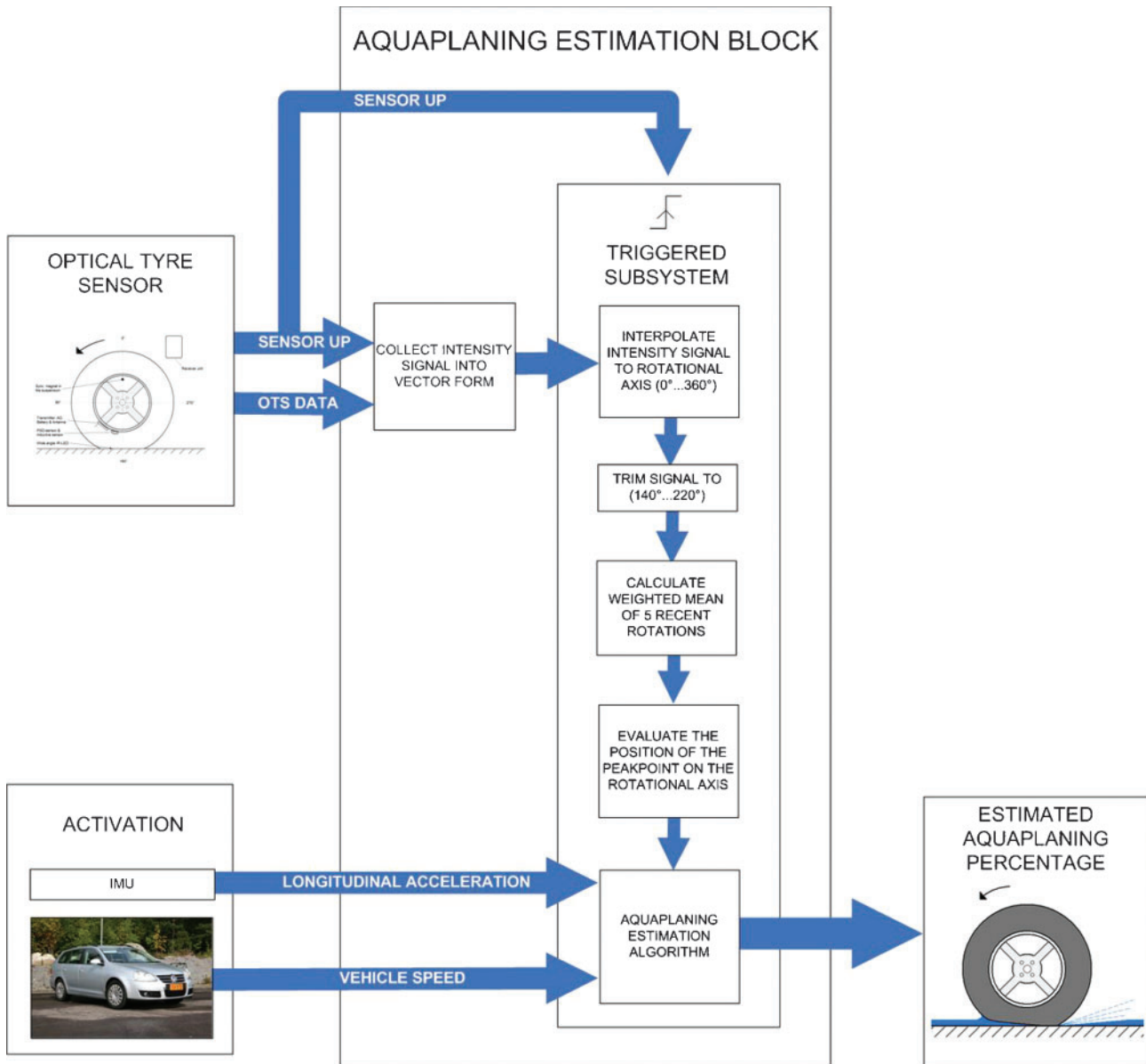


Fig. 6 Diagram of the whole real-time aquaplaning estimation process

where  $k = 0-360$  and  $l$  is the actual number of data points in the data vector of current rotation

$$z_{\text{input}}(k) = \text{floor}(e(k)) \quad (4)$$

$$z_{\text{input}}(k+1) = \text{ceil}(e(k)) \quad (5)$$

$$z_{\text{output}}(k) = z_{\text{input}}(k) + \frac{z_{\text{input}}(k+1) - z_{\text{input}}(k)}{l/360} \quad (6)$$

The most interesting part of the signal is around the contact area (rotation angles  $140-220^\circ$ ). The estimation exploits only this area of the signal. As can be seen from Fig. 4, this covers most of the information.

The signal is smoothed by calculating the weighted mean of five recent rotations. The number of rotations for the calculation and weighting coefficients were defined empirically to smooth the signal sufficiently and still give a sharp response. Equation (7) shows how the weighted mean of five recent rotations is calculated from stored data vectors

$$z_{\text{mean}} = \sum_{i=-4}^0 c_i z_i \quad (7)$$

where  $z_i$  are input vectors and  $c_i = [0.05 \ 0.10 \ 0.15 \ 0.20 \ 0.50]$  are weight coefficients.

The CM position is calculated from the  $z_{\text{mean}}$  vector by using the elements of the vector as mass

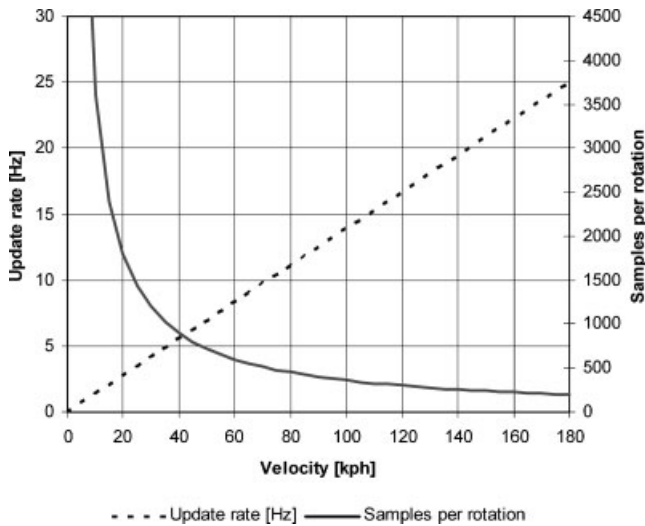


Fig. 7 Samples per rotation and update rate as a function of velocity, with a sampling rate of 5000 Hz

particles and the index number as position

$$CM = \frac{\sum_{i=140}^{220} (z_{mean,i} \cdot i)}{\sum_{i=140}^{220} z_{mean,i}} \quad (8)$$

where  $z_{mean,i}$  is the  $i$ th element of vector  $z_{mean}$ .

Figure 8 shows the determination of the aquaplaning percentage. As the CM position (equation (8)) of the  $z_{mean}$  vector shifts towards smaller rotation angles, the estimated aquaplaning percentage increases. The boundary points, where the aquaplaning percentages are 0 and 100 per cent, are determined empirically. When the vehicle is driven on dry tarmac at a constant speed, the CM position is around  $180^\circ$ , and in a full aquaplaning situation it is around  $174^\circ$ . Estimating the aquaplaning percentage in a linear fashion is only one method. There might be a better one for more accurate estimation.

The equation for calculating the estimated aquaplaning percentage is

$$p_{aqua} = \frac{100}{CM_{100} - CM_0} \times (CM - CM_0) \quad (9)$$

where the parameters are  $CM_{100} \approx 174^\circ$  and  $CM_0 \approx 180^\circ$ .

#### 4 RESULTS

The estimated aquaplaning percentage values with different speeds are shown in Fig. 9. The starting

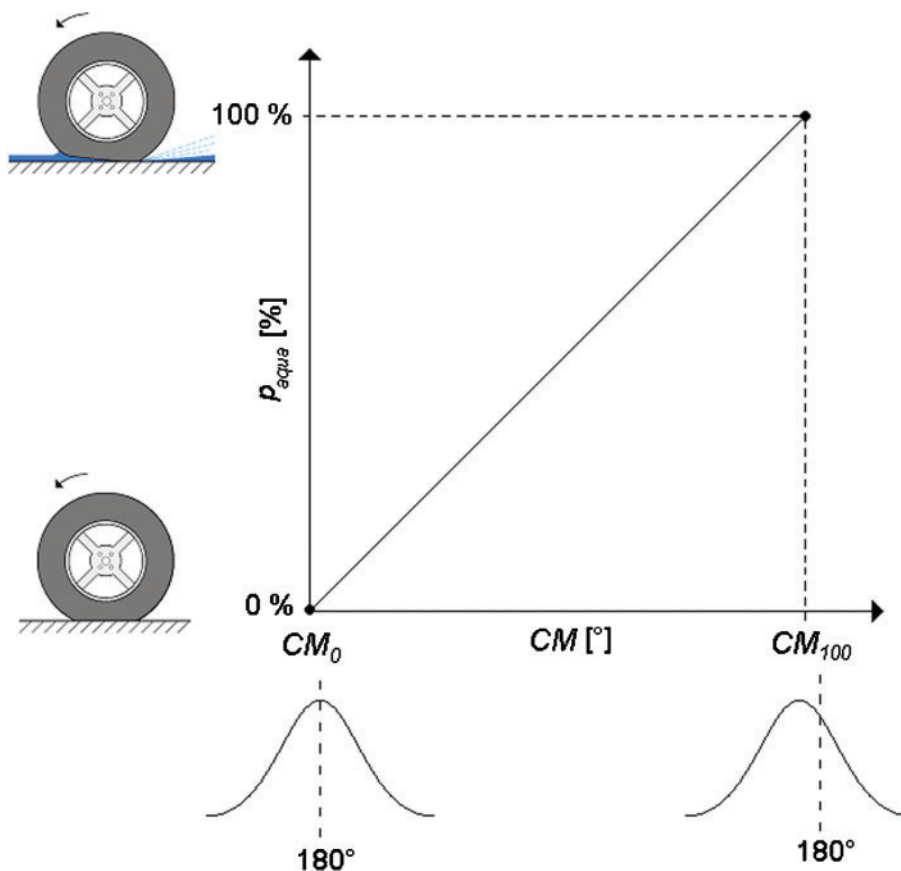


Fig. 8 Aquaplaning percentage determination

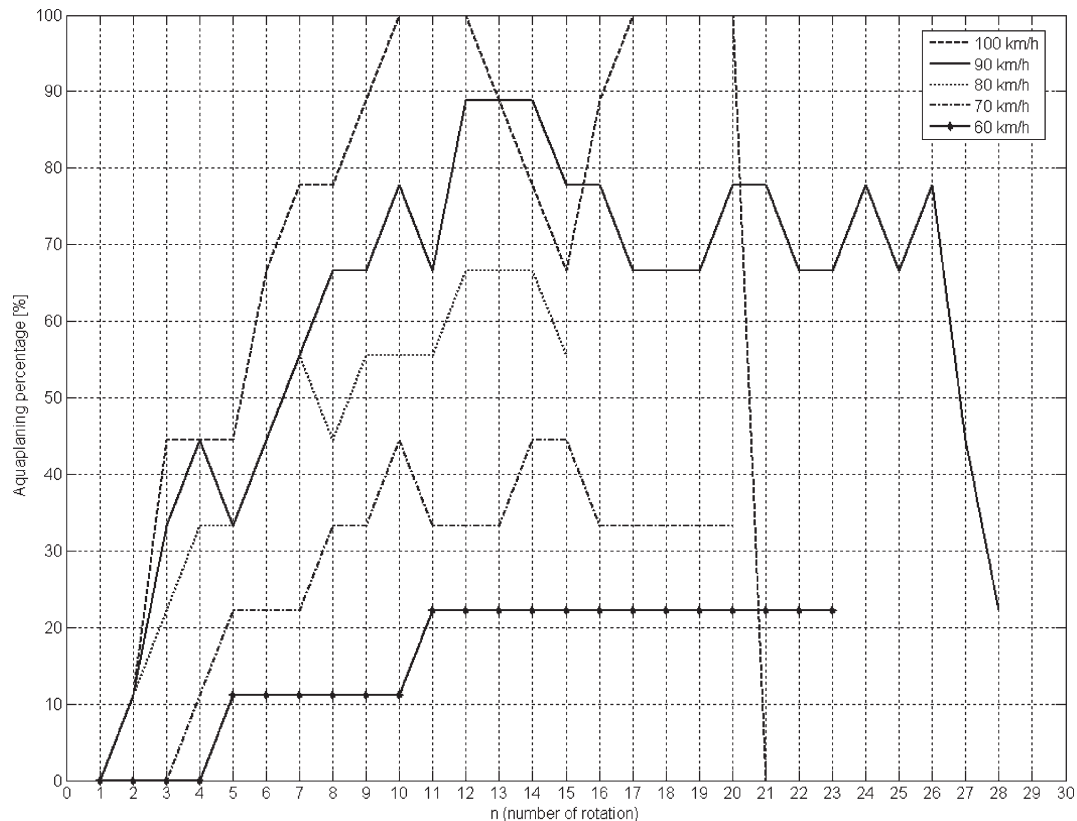


Fig. 9 Aquaplaning percentage with different vehicle speeds

point of the  $x$  axis (number of rotations) was defined from the clutch pedal information. The driver depressed the clutch pedal just before the tyre entered the water reservoir. Figure 9 shows that, even at a very slow speed, such as 60 km/h, the partial aquaplaning of the tyre can be detected. Figure 9 also shows how the estimated aquaplaning percentage rises quite linearly with the vehicle speed.

As can be seen from Fig. 9, the aquaplaning percentage increases gradually and there is also a lag at the beginning of each curve. The steps of the curves can be partly explained by the calculation and measurement method. The estimated aquaplaning percentage is calculated only once per rotation, and therefore it is updated once per rotation. The deviation of the estimated aquaplaning percentage can be explained by the dynamic nature of aquaplaning. The contact situation changes all the time during aquaplaning, and at some point the tyre can achieve more contact with the road surface. The lag at the beginning of the curves is probably due to the ramp of the water reservoir. Because of the ramp, the depth of the water at the beginning is less than it is in the rest of the water reservoir. The clutch pedal signal, which triggers the beginning of the water

reservoir, also has some deviation between test runs because it depends on the driver.

As a comparison with conventional methods, in Fig. 10 the longitudinal slip ratios  $\kappa$  are plotted in relation to the number of rotations of the tyre (the same test runs as in the aquaplaning percentage in Fig. 9). Figure 10 shows clearly that only the full aquaplaning situation (90–100 km/h) can be detected with wheel speed sensors. However, the feasibility of this information is questionable, because it can only detect severe and ongoing aquaplaning. At slower speeds the longitudinal slip does not give much information about aquaplaning. Additionally, the determination of the longitudinal slip is very sensitive to the actual ground speed, which cannot be directly measured in production cars.

## 5 DISCUSSION

The optical tyre sensor has proved that it can accurately measure the carcass deflection of a rolling tyre, which can be exploited in estimating aquaplaning in real time. The problem is that a braking situation has a similar effect on the vertical signal to

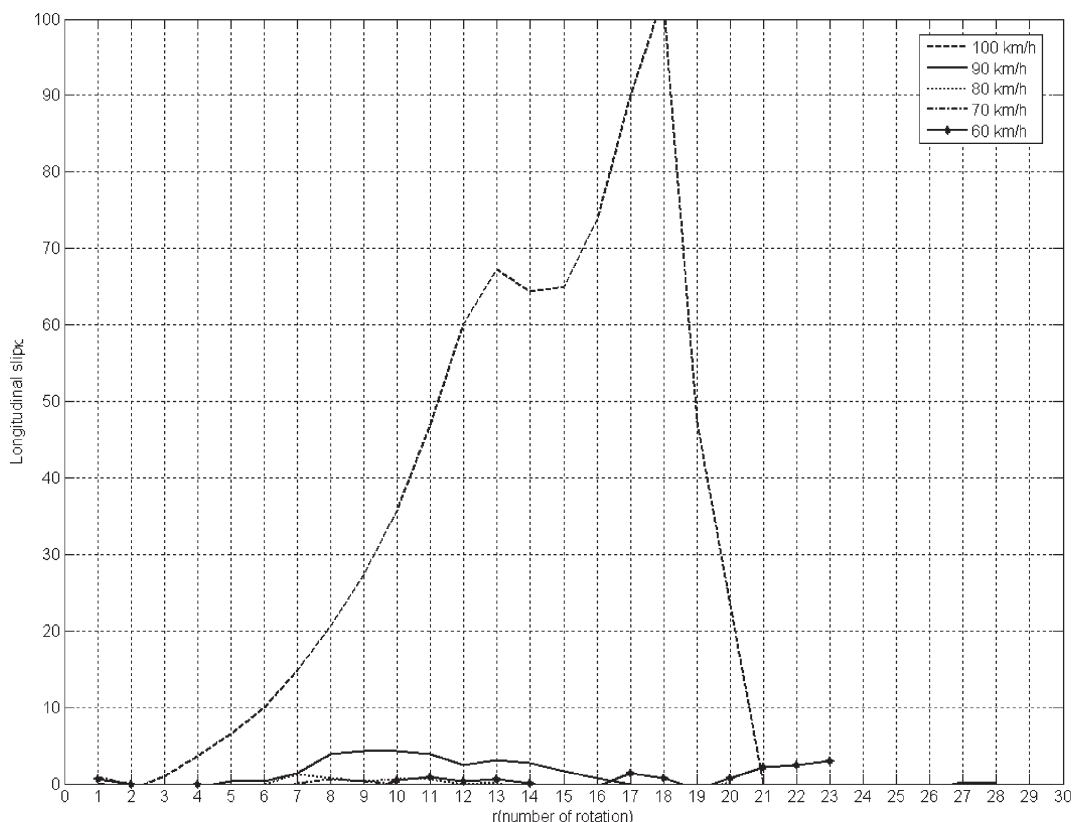


Fig. 10 Longitudinal slip at different speeds

aquaplaning, although the phenomena in these situations are different. In practice, the tyre moves circumferentially during braking, and this causes the peak point position of the signal to shift closer to the leading edge of the tyre on the rotational axis. However, with brake pressure information or longitudinal acceleration measurement, the braking situation can be filtered away from the aquaplaning situation.

The longitudinal signal of the OTS can also be exploited for the estimation of aquaplaning. By using both signals (the vertical and longitudinal signals of the OTS), the validity of the estimated aquaplaning percentage could be improved. Different algorithms could also be used. Estimating the aquaplaning percentage by comparing the standard deviation from 5–20 recent rotations of the vertical or the longitudinal signal was tested. However, it required all the data vectors to be saved to memory, which slowed the estimation and allocated too much memory space.

The real-time estimation of aquaplaning studies with the OTS is useful for future research and development projects with different types of sensor concept. There are various ways of estimating aquaplaning, and OTS is only one possible system

for this. A piezoelectric deformation sensor, inner liner strain sensor, or accelerometer could also be used for the estimation of aquaplaning. For instance, tests with OTS have shown that the hydrodynamic zone in aquaplaning (zone A, Fig. 1) vibrates, and this phenomenon could easily be sensed with an accelerometer.

#### ACKNOWLEDGEMENT

This work was financially supported by the EU project FRICTION FP6-IST-2004-4-027006. This support is gratefully acknowledged.

© Authors 2009

#### REFERENCES

- 1 Horne, W., Joyner, U., and Leland, T. Studies of the retardation force developed on an aircraft tire rolling in slush or water, NASA TN D-552, Washington, DC, USA, 1960.
- 2 Gough, V. E. Tire to ground contact stresses. *Wear*, 1958, 2(2), 107.
- 3 Herrmann, S. R. *Simulationsmodell zum Wasserabfluss- und Aquaplaning-Verhalten auf Fahrbahno-*

- berflächen*. Dissertation, Universität Stuttgart, Stuttgart, Germany, 2008.
- 4 **Tuononen, A.** and **Hartikainen, L.** Optical position detection sensor to measure tyre carcass deflections in aquaplaning. *Int. J. Veh. Syst. Modelling and Test.*, 2008, **3**(3), 189–197.
- 5 **Stöcker, J.** Erkennung inhomogener Kraftschlußverhältnisse zwischen Reifen und Fahrbahn am Beispiel Aquaplaning. *VDI Ber.*, 1993, **1088**, 345–369.
- 6 APOLLO Project: Intelligent tyre for accident-free traffic. Final report available from [www.vtt.fi/apollo](http://www.vtt.fi/apollo) (last accessed 3 March 2009).
- 7 **Tuononen, A. J.** Optical position detection to measure tyre carcass deflections. *Veh. Syst. Dynamics*, 2008, **46**(6), 471–481.
- 8 Hamamatsu PSD selection guide 2003, available from <http://www.hamamatsu.com/> (last accessed 6 March 2009).

## APPENDIX

### Notation

$c$	circumference of the tyre
$c_i$	weight coefficients of the weighted mean calculation
CM	centroid value (rotation angle) of the intensity signal

$CM_0$	empirically chosen centroid value of the intensity signal, where the tyre is not aquaplaning
$CM_{100}$	empirically chosen centroid value of the intensity signal, where the tyre is fully aquaplaning
$e$	index point value in the input vector for the polar coordinate system
$k$	index of the polar coordinate system
$l$	actual number of data points in the data vector of current rotation
$p_{\text{aqua}}$	estimated aquaplaning percentage
$r_d$	dynamic rolling radius of the tyre
$s_a$	samples attained per rotation
$s_r$	sample rate
$u_r$	update rate
$v$	velocity of the vehicle
$z_i$	interpolated intensity signal from one rotation
$z_{\text{mean}}$	weighted mean of the intensity signal from five previous rotations
$\kappa$	longitudinal slip